International Journal of Luminescence and applications
Vol6 (4) January, 2017, **ISSN 2277 – 6362**

Photoluminescence studies of Blue emission of $Y_2O_3:Eu^{2+}$ Nanophosphor

Nikhil R Jha[1] R K Kuraria[2]and P D Sahare[3]

[1]Department of Physics, Takshshila Institute of Engineering and Technology, Jabalpur, MP, India
[2]Department of Physics, Government Autonomous Model Science college, Jabalpur, MP, India - 482001
[3]Department of Physics & Astrophysics, University of Delhi, Delhi, India - 110 007
Corresponding author: nikhilr_jha@rediffmail.com: H/P0091 8989728943

Abstract *- The present paper reports the Photoluminescence of Eu^{2+} electronic transition of Y_2O_3:Eu Nanophosphor. The samples are prepared by combustion synthesis route. Urea is employed as fuel in this synthesis method. XRD results of samples were found to have cubic nanocrystalline structure ranging from 12-65nm which resembles with the TEM results. Research work explores the PL emission of 425nm corresponding to 374nm excitation of $Y_2O_3:Eu^{2+}$ Nanophosphor. Paper reports the effect of annealing temperature on PL intensity of $Y_2O_3:Eu^{2+}$ phosphor. 1931 CIE coordinates shows Eu^{2+}transition of Blue emission corresponding to coordinates x=0.1703, y=0.0057.*

Keywords: *PL excitation and emission*

1. INTRODUCTION

Trivalent Europium doped Y_2O_3 has been recognized as a prominent red emitting phosphor which has enormous applications [1]. Much studies are been done on the trivalent electronic transition of Eu^{3+} both on bulk and nanophosphors. Nanosize $Y_2O_3:Eu^{3+}$ is widely applied in the field displays (FED) and high definition Televisions (HDTV) [2-4]. The well known transition of Eu^{3+} is attributed to red emission at 611nm which is due to electronic transition from $^5D_0 \rightarrow {}^7F_2$.

Many different synthesis techniques such as sol-gel [5], spray pyrolysis method [6], CVD [7], co-precipitation [8, 9] methods have been reported for preparation of $Y_2O_3:Eu^{3+}$ nanoparticles and thin films. Comparative studies of different synthesis were done for the preparation of nanocrystalline $Y_2O_3:Eu^{3+}$ [11]. W. Chen et al. reported Morpology controlled synthesis of Y_2O_3:Eu [12]. Recently much work is done by M.G.Ivanov et al. with new laser synthesis [13] for preparation of nanoluminophors..

Combustion synthesis has been a common preparatory methods employed for nanoparticle preparation [14-16]. In our research we have employed combustion synthesis for preparation of nanophosphor.

This is the first time Eu^{2+} transition Y_2O_3 nanophosphor is reported in the present research work.

2. EXPERIMENT

Y_2O_3 (99.99%), E_2O_3 (99.99%), Nitric Acid (80% A.R.), Urea, Glycine, Citric Acid, Tartaric Acid, Oxalic Acid are taken as starting raw materials. $Y(NO_3)_3$ and $Eu(NO_3)_3$ stock solutions were prepared by dissolving Y_2O_3 and Eu_2O_3 in nitric acid and warming these solutions at 70-80^{0}C over the electric heater. Initially brown fumes evolve from the solution and after 10-15 mins vivid transparent solutions of nitrates are obtained.

For Combustion synthesis route the solution of $Y(NO_3)_3$ and $Eu(NO_3)_3$ were mixed according to the formula $(Y_{0.95},Eu_{0.05})_2O_3$ in a beaker and suitable amount of Urea or Glycine is added taking U/N molar ratio unity. The solution then heated with continuous stirring till the excess water evaporates leaving brownish yellow gel. The Gel is transferred into silica crucible and placed under preheated 600^0C furnace for 2.5 hours.

$$(2-2x)Y(NO_3)_3 + 2xEu(NO_3)_3 + 5(NH_2)_2CO \rightarrow (Y_{1-x}Eu_x)_2O_3 + 5CO_2 + 8N_2 + 10H_2O$$

$$6Y(NO_3)_3 + NH_2CH_2COOH \rightarrow 3Y_2O_3 + 20CO_2 + 20H_2O + 14N_2$$

The prepared sample is annealed at different temperatures 600, 850, 1000, 1200 and 1400ºC, so as to study the effect of temperature on $Y_2O_3:Eu^{2+}$ phosphor on PL intensity.

The morphology and particle size of prepared samples were observed by using X-Ray Diffraction Spectroscopy. The XRD measurements were carried out using Bruker D8 Advance X-ray diffractometer. The x-rays were produced using a sealed tube and the wavelength of x-ray was 0.154 nm (Cu K-alpha). The X-rays were detected using a fast counting detector based on Silicon strip technology (Bruker LynxEye dtector). PL testing is done on "Varian-CARY ECLIPSE Fluorescence Spectrophotometer" for Excitation and Emission slit width 1.5.

3. RESULTS AND DISCUSSION

XRD patterns of $Y_2O_3:Eu^{2+}$ nanophosphors are shown in shown in Fig. 1 for different annealing temperatures. Comparing the XRD data with standard JPDS data file 25-1011, it found to belongs to cubic crystal system. The broadening of the peaks (at FWHM) of prepared powders suggests particle smaller particle size in nm range. The size of the sample is estimated using Sherrer's formula: $D = (0.89\lambda)/(\beta\cos\theta)$, Where D is the average diameter of the grains, λ is the wavelength of X-Ray (= 0.1541nm), β is Full Width at Half Maximum (FWHM) of X-Ray diffraction lines and θ is Braggs angle. Particles are found to have particle size ranging from12-66nm for different temperatures from 600 to 1400ºC.

It is clear from the fig. 1 that particle size increase with the increase of annealing temperature. The XRD results match with TEM results. Fig. 2 shows the TEM image of particle annealed at 600ºC for 2.5 hours, which seem to have particle size ranging between 10-15nm.

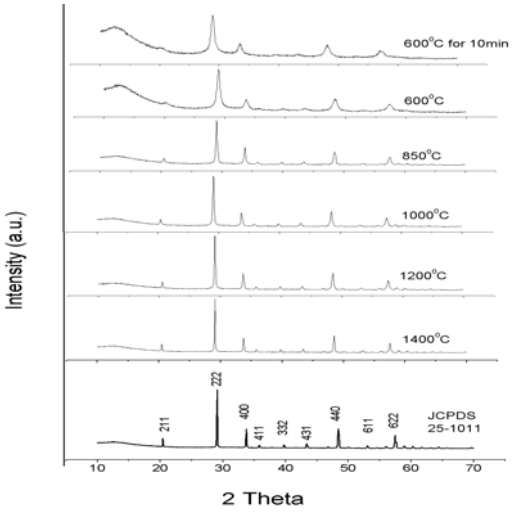

Fig. 1. Comparsion of XRD for different annealing temperature

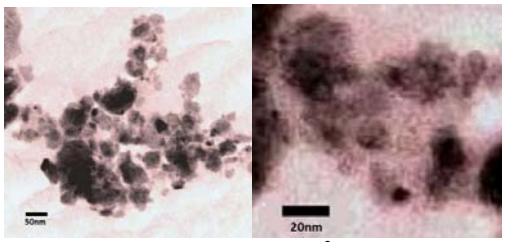

Fig 2. TEM images of $Y_2O_3:Eu^{2+}$ nanophosphors

Fig. 3 Shows the PL emission and excitation corresponding to 425nm and 374nm respectively of Y_2O_3:Eu. Figure shows that both the peaks are identical in PL spectrum, which proves, vice-versa emission and excitation at 425nm and 374nm wavelength.

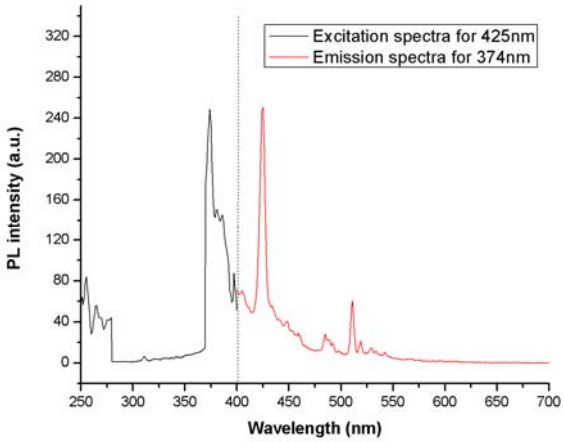

Fig 3 Identical PL spectra for Emission and excitation of $Y_2O_3:Eu^{2+}$ (λ_{ex}=374nm and λ_{em} = 425nm)

The emission of 425nm is probably due to Eu^{2+} transition between $4f^{7+}$ and $4f^{6}5d^{1}$ of electron in Y_2O_3:Eu nanophosphors for respective excitation and emission wavelengths. [23-25 17-19].

The absorption and emission spectra of divalent Europium are due to electronic transitions between the $4f^{7+}$ and $4f^{6}5d^{1}$ electronic configurations shown in Fig. 4. [26 20]. The strongest lines were actually assigned to pure electronic transitions from $4f^{n}$ to $4f^{n-1}5d$ which was assumed to be caused by the interaction between the $4f^{n-1}$ core and the 5d electron, the $4f^{n-1}5d$ level being spaced with the energy gaps in the $4f^{n-1}$ ground multiplets [24, 18]. An approximate energy level scheme was proposed (Blasse et al. 1968) for the electronic transitions in Eu^{2+} by using strong field formalism to describe the 5d levels and the weak field formalism to describe the 4f orbitals.

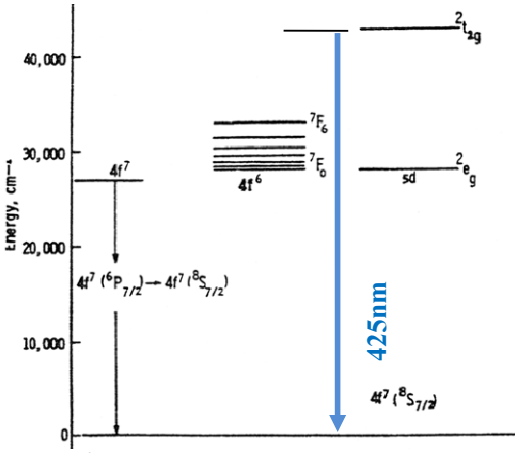

Fig. 4 Eu^{2+} transition in Y_2O_3:Eu nanophosphor

The ground state of Eu^{2+} is $^{8}S_{7/2}$ because of the $4f^{7}$ electronic configuration. In the configuration $4f^{6}5d^{1}$, one electron occupies a 5d orbital which is splited into two orbital sets sub-levels $^{2}t_{2g}$ and $^{2}e_{g}$ (upper sublevel is $^{2}t_{2g}$ and Lower sublevel is $^{2}e_{g}$ shown in fig 4) , by a cubic crystal field. Thus the energy terms are $^{2}e_{g}$ and $^{2}t_{2g}$ in full cubic symmetry.

The Y_2O_3 lattice dependence of the emission color of the Eu^{2+} is mainly connected with covalence (the nephelauxetic effect), which will reduce the energy difference between the 4f and 5d configurations, crystal field splitting of the 5d configuration and the Stokes shift (Blasse and Grabmaier 1994).

The transition of Eu^{2+} shows two energy sub-levels $^{2}t_{2g}$ and $^{2}e_{g}$ splitted at $5d^{1}$ energy level. It is evident that the lower energy sub-level transition will be from $4f^{6}5d^{1}(^{2}e_{g})$ to $4f^{7}$ ($^{8}S_{7/2}$) which will emit higher wavelength emission in comparison to the transition from higher energy sub-level $^{2}t_{2g}$ to ground state $^{8}S_{7/2}$. This is a well seen small peak at higher wavelength at 526nm. Hence we conclude that the 425nm (blue) Emission is due to transition from $4f^{6}5d^{1}(^{2}t_{2g})$ to $4f^{7}$ ($^{8}S_{7/2}$) *(from upper energy level $^{2}t_{2g}$ to ground state $^{8}S_{7/2}$)*. Also it is evident from XRD results that the prepared samples are **cubic**.

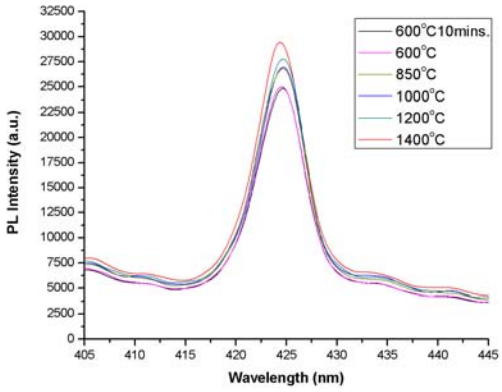

Fig. 5 PL spectra of Y_2O_3:Eu^{2+} nanophosphor annealed at different temperature

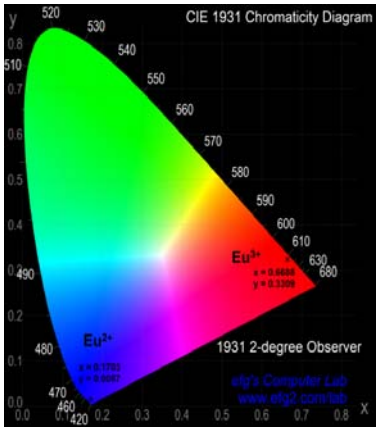

Fig. 6 CIE coordinates depicted on 1931 chart where x = 0.1703, y = 0.0057 and x = 0.6688, y= 0.3309 for 425nm of $Eu^{2+}$and 611nm of Eu^{3+} (5%) doped Y_2O_3 nanophosphor respectively

Fig. 5 shows the effect of temperature on PL intensity of Y_2O_3:Eu^{2+} nanophosphor. It is found that the PL intensity increases with the increase of temperature which is evident that is due to increase of particle size.

Fig 6 Shows the CIE coordinates of 425nm emission and 611nm emission of Y_2O_3:Eu^{2+} and Y_2O_3:Eu^{3+} nanophosphor. 1931 CIE coordinates shows 425nm emission in blue color region.

REFERENCES

1. S. Schionoya, W. M. Yen, Phosphors Handbook, CRC Press, New York, 1999.

2. A. Vccht, C. Gibbons, D. Davies, X. Jing, P. Marsh, T. Ireland, J. Silver, A, Newport, D. Barber, J. Vac. Sci. Technol. B17 (1999) 750
3. X. Jing, T. Ireland, C. Gibbons, D. J. Barber, J. Silver, A. Vecht, G. fern, P. Trowga, D. C. Morton, J. Electrochem. Soc. 146 (1999) 4654
4. M.H. Lee, S.G. Oh, S.C. Yi, D.S. Seo, J.P. Hong, C.O. Kim, Y. K. Yoo, J.S. Yoo, j. Electrochem. Soc. 147 (2000) 3139
5. S. Alaruri, T. Bonsett, A. Brewington, E. Mepheeters, M. Wilson, J. Mater. Res. 14 (1999) 2611.
6. A. Konard, T. Fries, A. Gahn, F. Kummer, U. Herr, R. Tideeks, K. Samwer, J. app. Phy. 86 (1999) 3129
7. R. Schmechen et al., J. Appl. Phys, 89 (2001) 1679
8. D. Ma, X. Liu, Y. Pei, L. Cao, SID 97 (1997) 423.
9. M. Kabir, M. Ghahari, and M. Shafiee Afarani, Ceramics International, vol. 40, no. 7, (2014) pp. 10877–10885
10. T. K. Anh, L.Q. Minh, N. Vu et al., J. Lumin, 102-103 (2003)
11. Nikhil R Jha, R K Kuraria, S R Kuraria and P D Sahare, International Journal of Luminescence and applications Vol5 (4) December, 2015, pages 500-505
12. W. Chen, Y. Tong, Y. Liu et al., Ceramics International, vol. 39, no. 4, pp. 3741–3745, 2013.
13. M. G. Ivanov, U. Kynast, and M. Leznina, Proceedings of the International Conference on Luminescence and Optical Spectroscopy of Condensed Matter (ICL ’14), Wroclaw, Poland, July 2014
14. T. K. Anh. L. Q. Minh, N. Vu, et al. J. Mater, Pro. Tech. 121 (2002) 265
15. Nguyen Vu, T. K. Anh, G. C. Yi, W. Strek, J. of Lumin. 122-123 (2007) 776-779
16. Tran Kim Anh Pham ThiMinh Chau, Nguyen Thi Quy Hai, and Le QuocMinh, Journal of Nanomaterials, Volume (2015), Article ID 637124, 7 pages
17. P Dorenbos, Journal of Luminescence, Vol. 104, Issue 4, Aug 2003, Pg 239-260
18. Lucas, F., Jaumes, S., Quarton, M., LeMercier, T., Guillen, F., Fauassier, C. J. Solid State Chem. 2000, 150, 404
19. Chia-Pin Lin, Sheng-Tsong Chen and Teng-Ming Chen; Tankang Journal of Science & Engineering, Vol. 5, No.2, pp 81-84, 2002
20. Book “Luminescence Spectroscopy of Minerals and Materials”, Michael Gaft, Renata Reisfeld and Gerard Panczer, Springer-Verlag, Berlin Heidelberg 2005, Printed in Germany.